LBL-16390 c.2

Lawrence Berkeley Laboratory
UNIVERSITY OF CALIFORNIA

RECEIVED
LAWRENCE
BERKELEY LABORATORY
SEP 27 1983
LIBRARY AND
DOCUMENTS SECTION

To be presented at the International Conference on Nuclear Physics, Florence, Italy, August 29 - September 3, 1983

STATISTICAL PROPERTIES OF DEEP INELASTIC REACTIONS

L.G. Moretto

August 1983

LBL-16390 c.2

Prepared for the U.S. Department of Energy under Contract DE-AC03-76SF00098

DISCLAIMER

This document was prepared as an account of work sponsored by the United States Government. While this document is believed to contain correct information, neither the United States Government nor any agency thereof, nor the Regents of the University of California, nor any of their employees, makes any warranty, express or implied, or assumes any legal responsibility for the accuracy, completeness, or usefulness of any information, apparatus, product, or process disclosed, or represents that its use would not infringe privately owned rights. Reference herein to any specific commercial product, process, or service by its trade name, trademark, manufacturer, or otherwise, does not necessarily constitute or imply its endorsement, recommendation, or favoring by the United States Government or any agency thereof, or the Regents of the University of California. The views and opinions of authors expressed herein do not necessarily state or reflect those of the United States Government or any agency thereof or the Regents of the University of California.

Statistical Properties of Deep Inelastic Reactions

L.G. Moretto

Nuclear Science Division, Lawrence Berkeley Laboratory,

University of California, Berkeley, California 94720

This work was supported by the Director, Office of Energy Research, Division of Nuclear Physics of the Office of High Energy and Nuclear Physics of the U.S. Department of Energy under Contract DE-AC03-76SF00098.

LBL-16390

Statistical Properties of Deep Inelastic Reactions

L.G. Moretto

Nuclear Science Division, Lawrence Berkeley Laboratory
University of California, Berkeley, CA 94720

Abstract: The multifaceted aspects of deep-inelastic heavy-ion collisions are discussed in terms of the statistical equilibrium limit. It is shown that a "conditional" statistical equilibrium, where a number of degrees of freedom are thermalized while others are still relaxing, prevails in most of these reactions. The individual degrees of freedom that have been explored experimentally are considered in their statistical equilibrium limit, and the extent to which they appear to be thermalized is discussed. The interaction between degrees of freedom on their way towards equilibrium is shown to create complex feedback phenomena that may lead to self-regulation. A possible example of self-regulation is shown for the process of energy partition between fragments promoted by particle exchange.

Introduction

Statistical mechanics, undoubtedly a pinnacle of scientific achievement, was spawned by the 19th century extension of the illuministic tradition as an embarassing illegitimate offspring. The firm belief in a nature where integrability was the rule rather than the exception created a strongly biased view towards the problem of ergodicity. Chaos and randomicity were introduced more or less as "ad hoc" assumptions to accommodate a devious and reluctant nature, and the concept of ensembles betrayed the underlying belief that each element of an ensemble could not escape from the constraints imposed by the elusive "first integrals".

The modern renaissance of classical mechanics is about to make amends for the past and the legitimization of statistical mechanics is, to all practical purposes, about to be accomplished. Exponential instabilities, frequency doubling, strange attractors, and associated lexicon have made their appearance in the headlines of Physical Review Letters and in the fashionable quarters of physics. From this remarkable development we have learned two lessons. The first is that chaotic or random behavior can be achieved in extremely simple systems with apparently innocent nonlinear couplings; the second is that the evolution towards chaos does not necessarily occur smoothly but may be associated with interesting phenomena of self-organization, as in oscillating chemical reactions where feedback and self-regulation features seem to appear almost miraculously.[1)]

Statistical features were observed in nuclear systems very early in the development of nuclear physics. The understanding of the neutron resonance spacings and partial widths reaches deeply into the complexities of quantum statistical mechanics, while the theory of particle evaporation from a compound nucleus shows the elegant simplicity of the thermodynamic answers to apparently

complex questions. At present the statistical theory of compound nucleus is accepted as a "classical" chapter of nuclear physics.

The advent of heavy-ion reactions has opened a vast new area where much broader and more complex features seem to be amenable to a statistical treatment of some sort. Widely different relaxation times associated with different degrees of freedom are responsible for extensive phenomena of partial equilibration.[2] In other words, a number of nearly equilibrated modes appears to coexist with other modes that are still far from equilibrium. The understanding of these features has developed along two obvious lines. On one hand, the totally relaxed modes have been dealt with in terms of equilibrium statistical mechanics. Such an approach has been quite successful in describing (or at least in approaching) a rather complex and rich variety of phenomena. From an aesthetic point of view one cannot help but marvel at the striking increase in richness of the phenomenology as one moves from a mononuclear system (compound nucleus) to the dinuclear system associated with heavy-ion collisions. On the other hand, the partially relaxed modes have been treated in the framework of nonequilibrium statistical mechanics in terms of transport theories of various sorts.[3-6] This is, of course, a more ambitious undertaking as it requires a more detailed understanding of the dynamical properties of the system. The appreciation of this problem has led to a more profound study of the potential energy involved in the physics of fusion and reseparation,[7] as well as of the complex and hitherto unknown viscoelastic properties of nuclear systems.[8] The possibility that one-body properties dominate not only the static but also the dynamic behavior of the system is particularly interesting with regard to the latter point.[5,7] If this is borne out experimentally, we shall be confronted with a rather unique form of matter where viscoelastic properties depend not only on its bulk properties but on its surface boundary conditions as well. It is easy to prophesy that this point will be heavily explored in the immediate future.

In the limited space/time available here, I shall try to quickly survey the landscape of deep-inelastic processes from the "minimal" point of view of equilibrium statistical mechanics with occasional forays into the time-dependent regime when some point appears to be worth making. In particular, in the case of the coupling between mass exchange and energy dissipation, I shall point out the exciting possibility of feedback and self-regulatory phenomena that have not been considered so far. As a general approach, I shall consider a list of degrees of freedom that experiment has shown to be relevant, I shall discuss the expectations in terms of equilibrium statistical mechanics, and I shall confront such results with the available experimental data. Inevitably a lot of exciting developments will be given the brush-off or will be altogether forgotten in such presentation. Hopefully, these sacrifices will help to make the presentation more intelligible if not more interesting to a broader audience.

A brief reminder of the mononuclear case

The statistical studies that can be performed with a compound nucleus are relatively few indeed, although quite important. On one hand, we have the measurement of the level density and of the fluctuations in level widths and spacings. On the other, we have the classical evaporation experiment. If a compound nucleus is allowed to evaporate, what is the particle and energy distribution

of the "vapor" in equilibrium with the residual nucleus? The answer to this problem is quite straightforward. In particular, if one neutron at most can be evaporated from the nucleus, the energy distribution is $\rho(\varepsilon) \propto \sqrt{\varepsilon}\ e^{-\varepsilon/T}$ while the probability of emission of a particle with energy ε is $P(\varepsilon) \propto \varepsilon\ e^{-\varepsilon/T}$. Experimental results show that the statistical predictions are beautifully verified in many instances.

The dinuclear case

The variety of the thermodynamical features that are potentially observable increases dramatically as one goes from the mononuclear case to the dinuclear case. We can immediately see that a large number of microscopic or thermodynamic degrees of freedom can be called into play. Let us mention some of the associated problems, which we are going to consider in some detail.

a) Given a fixed amount of energy made available to the internal degrees of freedom of the system, what is the resulting partition of energy between the two fragments?

b) If the two nuclei are allowed to change their mass, what is the resulting mass distribution?

c) If the two nuclei are constrained to a fixed mass, what is the distribution in the neutron-to-proton ratio?

d) Finally, if the system is given a fixed amount of total angular momentum, what is the resulting distribution of the components of the angular momentum in each of the fragments?

We can give a straightforward answer to each of these questions in the limit of statistical equilibrium, and we can verify to what extent nature complies with these predictions.

e) A problem related to d) is the angular distribution of the products. While the role of statistical mechanics in this problem is not unique and not necessarily dominant, we shall illustrate some interesting interplay between statistical and quantum mechanics in the determination of the shape of the angular distributions.

a) The energy partition between fragments

Two nuclei of mass A_1, A_2 are given an amount of energy E to share. Let us calculate the statistical weight of an arbitrary partition x and E - x to be assigned to fragment 1 and 2, respectively. The statistical weight is, of course, the overall number of states associated with this partition, which is clearly equal to the product of the level densities[9]:

$$P(x) = \rho_1(x)\ \rho_2(E - x) \tag{1}$$

The most probable partition can be obtained from the condition

$$\frac{d}{dx}\ \ell n\ P(x) = 0 = \frac{d}{dx}\ \ell n\ \rho_1(x) + \frac{d}{dx}\ \ell n\ \rho_2(E - x) = \frac{1}{T_1} - \frac{1}{T_2} \tag{2}$$

$$\text{or } T_1 = T_2 = T$$

The equality of the temperatures implies that the energy is divided proportionally to the mass of the fragments (if the fragments can be assumed to be two homogeneous pieces of the same substance)

$$\frac{x}{E-x} = \frac{A_1}{A_2} \tag{3}$$

Otherwise $\frac{x}{E-x} = \frac{C_{V1}}{C_{V2}}$

The variance of the distribution can also be easily calculated:

$$\frac{1}{\sigma^2} = -\frac{d^2}{dx^2} \ln P(x) = \frac{d}{dx}\left(\frac{1}{T_1}\right)_T + \frac{d}{dx}\left(\frac{1}{T_2}\right)_T = \frac{1}{T^2}\left(\frac{1}{C_{V1}} + \frac{1}{C_{V2}}\right) \tag{4}$$

The quantities C_{V1}, C_{V2} are the heat capacities of the two fragments. For a homogeneous Fermi gas $C_V = 2aT$, where a is the level density parameter. The variance is therefore

$$\sigma^2 = 2T^3 \frac{a_1 a_2}{a_1 + a_2} \tag{5}$$

The first prediction appears to be verified by experiment beyond any reasonable expectation. Not only does the energy divide proportionally to the mass when all the energy available has been dissipated[10,11] (namely for fully relaxed or fully damped events), but it does so also for incompletely relaxed events where only a fraction, at times quite small, of the available kinetic energy has been dissipated.[12-14]

In fig. 1 the preevaporation masses A* as well as the mean number of neutrons ν_n are given as a function of the preevaporation charge Z* for the reaction 340 MeV ^{40}Ar + Ag.[10] Masses

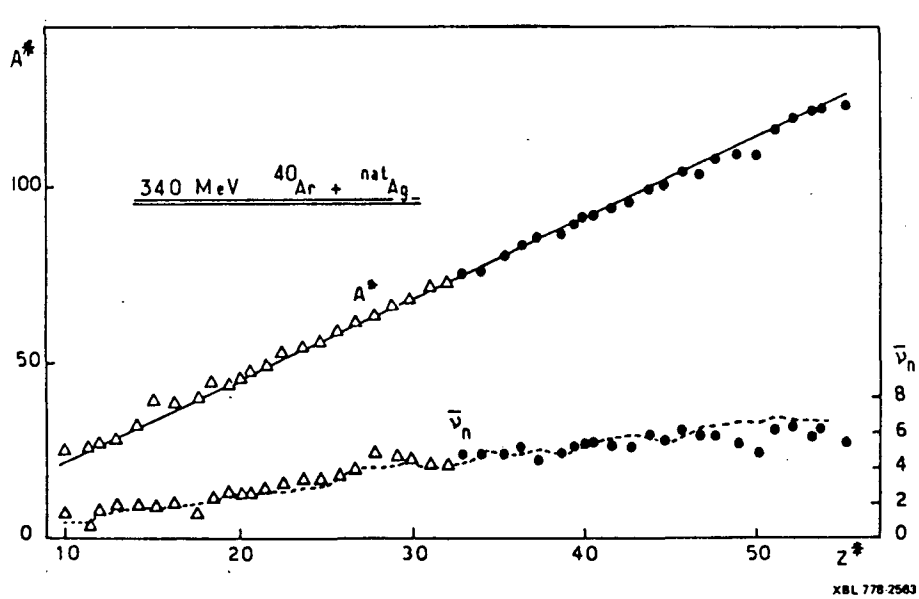

Fig. 1. Pre-evaporation masses A* (upper points) and average number of evaporated neutrons $\bar{\nu}_n$ (lower points). The dashed line is an evaporation calculation assuming an energy partition proportional to the masses.[10]

and neutron numbers are obtained from a kinematic analysis of the experiment. The dashed line is an evaporation calculation performed assuming an energy partition proportional to the preevaporation masses. The very good reproduction of the data proves the isothermicity of the fragments for fully relaxed collisions.

Similar results are obtained by a direct measurement of the neutrons emitted by the fragments.[12-14] Figure 2a shows the isothermicity of the neutron spectra emitted by complementary fragments; fig. 2b shows the equality of the ratio of the emitted neutrons to the ratio of the masses; fig. 2c shows that the ratio of the emitted neutrons is practically independent of the energy loss, suggesting fragment isothermicity at all Q-values.[12] Concerning the variance, no direct experimental evidence is available as yet. What is needed is, for instance, a correlated measurement of the neutrons emitted by both fragments. The presence of fluctuations in the energy partition should appear as a strong inverse dependence of the mean number of neutrons emitted by one fragment as a function of the number of neutrons emitted by the other. A Monte Carlo simulation[9] of this experiment is shown in fig. 3.

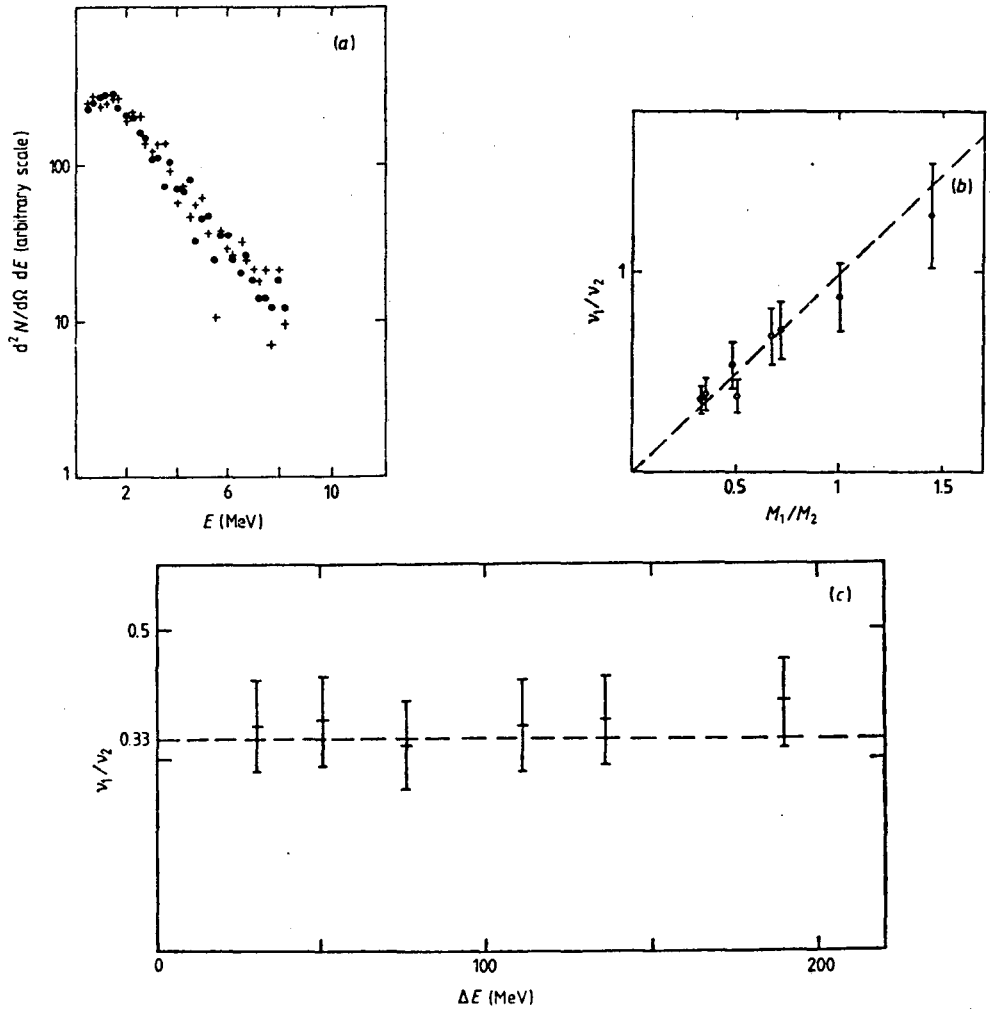

Fig. 2. Neutron emission in the reaction 400 MeV Cu + Au.[12] Top left: neutron kinetic energy spectra from the two fragments; top right: neutron multiplicity ratio as a function of mass asymmetry; bottom: neutron multiplicity ratio at fixed mass asymmetry (dashed line) as a function of energy loss.

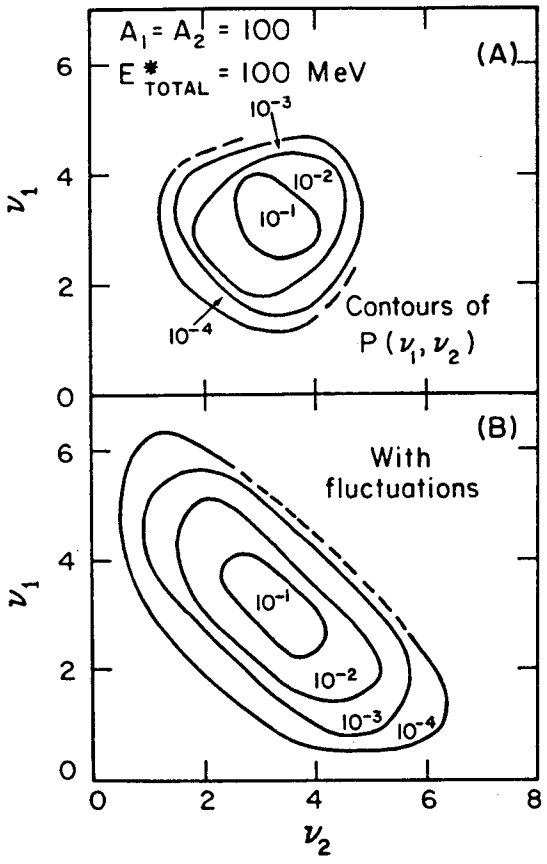

XBL 808-1552

Fig. 3. Probability distribution for the number of neutrons emitted by the two fragments for a Q-value of -100 MeV. The fluctuations in the energy partitions are incorporated in B.[11)]

Some indirect evidence of these energy fluctuations has been inferred from the high-energy tail of the proton spectra emitted in coincidence with the deep inelastic fragments in the reaction 252 MeV ^{20}Ne + Cu.[15)] The energy fluctuations between the two fragments in contact can lead to strong variations in the excitation energy (and thus in the temperature) of the Ne-like fragment, which are manifested in a more energetic energy tail of the proton spectrum (fig. 4).

While we may be well pleased by the simplicity of the statistical result and by its pervading success, we cannot dismiss the question: how does nature manage to obtain such an extensive thermalization in the short times indicated by the Q-value intervals under consideration ($\sim 10^{-21}$ s)? We shall deal with this question extensively later on.

b) <u>The mass distribution</u>

Two nuclei in contact can be characterized by the potential energy:

$$V(A_1) = E_{LD}(A_1, Z_1) + E_{LD}(A_2, Z_2) + E_{Prox} + E_{Coul} + E_{Rot} \qquad (6)$$

where E_{LD} are the liquid drop masses, E_{Prox} is the nuclear interaction between the two nuclei, E_{Coul} is the Coulomb interaction, and E_{Rot} is the rotational energy. A plot of this potential energy vs A_1 for various angular momenta is shown in fig. 5.

The topology of these energy surfaces has been extensively discussed with regard to the fission problem. For us it suffices to observe that, for rather heavy systems, the potential shows a minimum at symmetry and two maxima at intermediate asymmetries. A

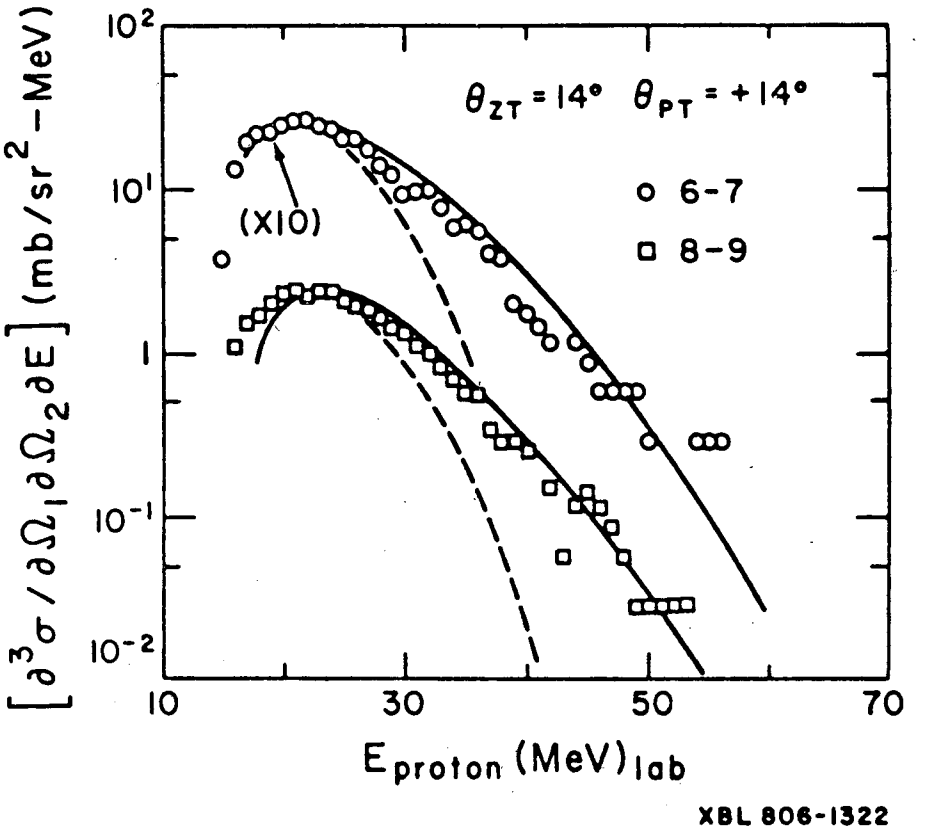

Fig. 4. Proton kinetic energy spectra in coincidence with a light fragment in the reaction Cu + ^{20}Ne at 252 MeV bombarding energy.[15] The dashed lines are calculations peformed using a fixed energy sharing proportional to the masses, while the solid lines allow for thermal fluctuations in the energy partition.

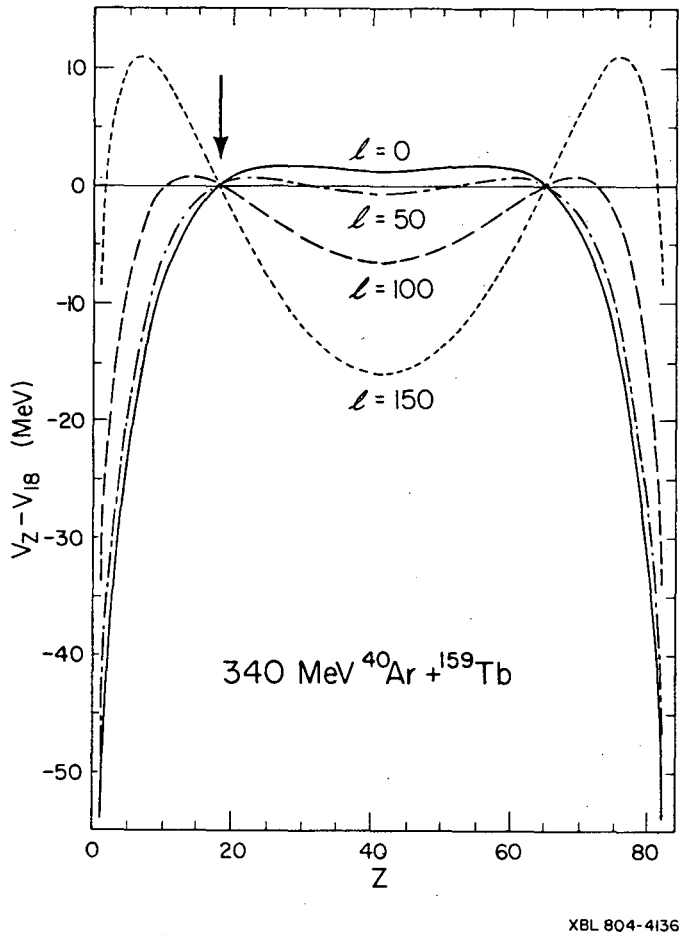

Fig. 5. Potential energies vs mass asymmetry (fragment atomic number) for various ℓ-waves for the system 340 MeV $^{40}Ar + ^{159}Tb$.

scission equilibrium model would lead to a mass distribution of the form:

$$P(A_1) \propto e^{-V(A_1)/T} \tag{7}$$

This form has a symmetric, fission-like peak and a light (and heavy complement) evaporation tail. Such a distribution is qualitatively reproduced in the fission and evaporation decay of compound nuclei, though the fission-like peak results from an oversimplified treatment that does not include the effect of the saddle-to-scission descent nor of shell and/or deformation energies. Nonetheless, it is legitimate to wonder whether a tendency towards equilibration of the masses near scission is visible in deep inelastic collisions.

The typical mass distributions are characterized by a target and projectile-like peaks plus a symmetric peak, which may or may not be present, and which is due at times to ordinary fission but more frequently to a process bypassing the compound nucleus stage and called fast-fission. The symmetric peak does indicate an extensive equilibration presumably occurring near scission. Some understanding of the conditions leading to such a process seems to have been obtained in Swiatecki's theory of fission and reseparation.[7] On the other hand, the deep inelastic peaks seem to be solidly anchored to the initial asymmetry without any indication of evolution towards symmetry. This is more evident when we look at the dependence of the mass asymmetry on energy loss as exemplified in fig. 6. We see that the entrance-channel mass asymmetry persists with increasing energy dissipation despite the presence

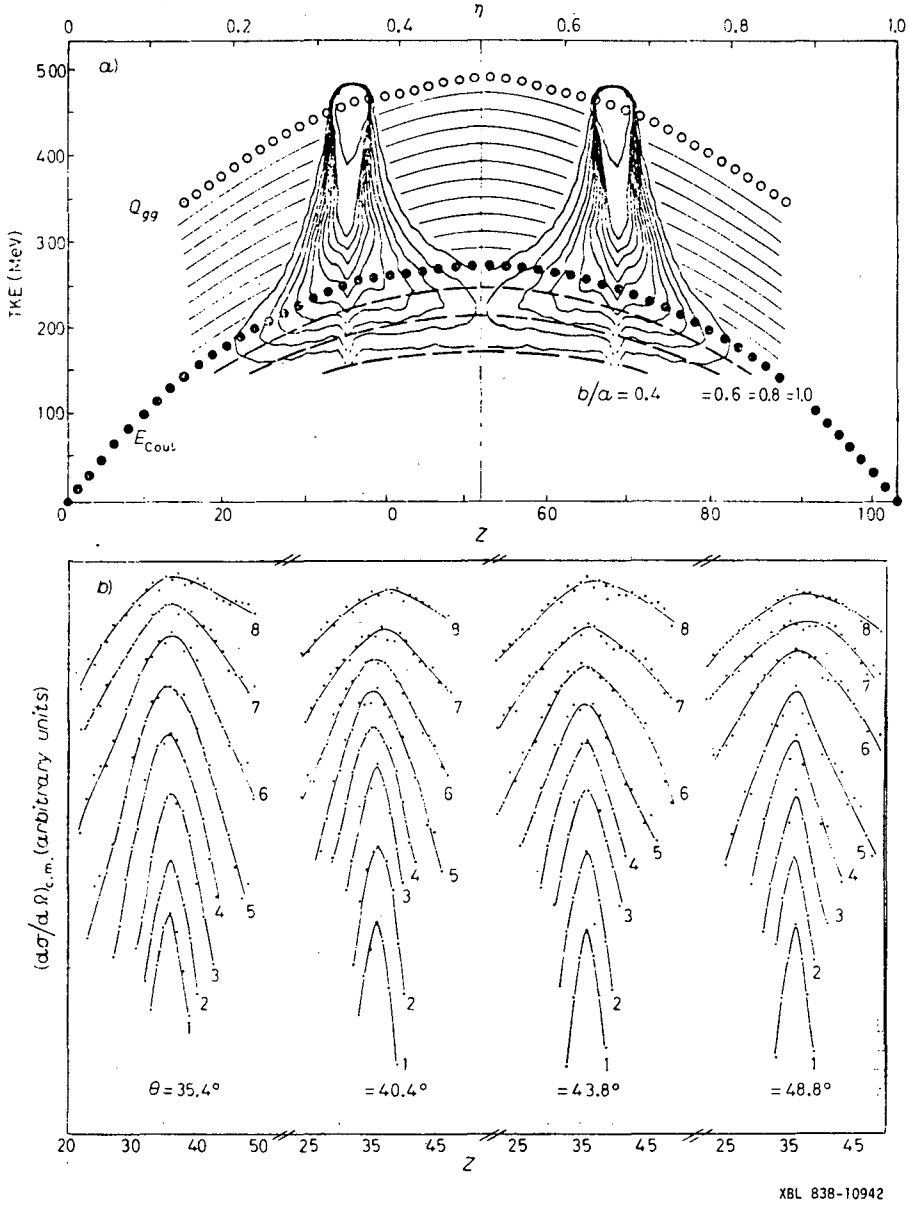

Fig. 6. a) Contour plot of the cross section in the total kinetic energy-atomic number plane for the reaction ^{86}Kr + ^{166}Er. The parallel lines between E_{Coul} and Q_{gg} are 20 MeV apart.[16] b) Center-of-mass charge distributions for various kinetic energy bins at various labortory angles in the reaction ^{197}Au + ^{86}Kr. The energy bins start 50 MeV below the Coulomb barrier of two touching spheres and increase in steps of 25 parallel to the Coulomb barrier.[17]

of strong driving forces towards symmetry. Only at the greatest energy losses, when the relative motion is totally damped, one observes a tendency of the system to move in the direction of the driving force. The lack of response of the system to the driving force towards symmetry is puzzling. Its causes can be searched in the inertia or in the friction associated with this mode or in some more complex dynamical effects. Be as it may, the reluctance of the mass asymmetry to equilibrate is as remarkable as the ability of the dissipated energy to reach a thermal distribution between the two fragments. In fact, these two apparently contradictory features may have a heretofore unsuspected relation.

Correlation and self-regulation in the dissipative particle exchange process

We have already commented on the remarkably rapid thermalization of the dissipated energy on one hand and on the reluctance of the mass asymmetry to move towards equilibrium on the other. We shall show here that the two relevant degrees of freedom are strongly coupled together and that such a coupling, rather than allowing the two modes to relax smoothly towards equilibrium, leads to a complex behavior of self-regulation.

The most obvious coupling between energy dissipation into each individual fragment and the mass asymmetry is the process of particle exchange. This coupling can be evidentiated in the correlation between the energy loss and the variance of the mass distribution.

The energy loss per particle exchanged is given by $\Delta E = \frac{m}{\mu} E$ where m is the particle mass and μ is the reduced mass, while the variance, assuming a random walk, is given by $\sigma^2 = N$, where N is the number of exchanged particles. A classical calculation along these lines substantially underpredicts the energy loss for any given value of σ^2 if nucleons are assumed to be the exchanged particles. The inclusion of the Pauli blocking in σ^2 and not in the energy loss, as required by the fact that the former quantity is the expectation value of a two-body operator while the latter is the expectation value of a one-body operator, seems to reproduce the data satisfactorily.[18] This agreement, shown in fig. 7, single-handedly proves that the particles exchanged are nucleons and manifests one of the very rare macroscopic quantal effects in the field of deep-inelastic processes.

What the experiment seems to prove is that a) there is mass transfer, b) that the mass transfer is associated with nucleon exchange, and c) that the nucleon exchange accounts for a good fraction of the dissipated energy.

Let us now turn to the self-regulatory effects that may be associated with the coupling of the two degrees of freedom.[19]

The obvious coupling, as we have seen, is the particle exchange, as it is naturally involved in the evolution of the fragment masses on one hand, and it is thought to be the major, if not the entire cause of energy dissipation on the other.[18] For simplicity, in our explanation we shall assume that: 1) particle exchange is the only means of energy transfer; and 2) intranuclear equilibration is immediate. We shall also assume that the particle fluxes are substantially temperature-dependent, as is clearly the case when a sufficiently high barrier is present between the two potential wells. This regime in fact prevails when the nuclear overlap is incomplete, which is also when the energy is dissipated most rapidly.[19]

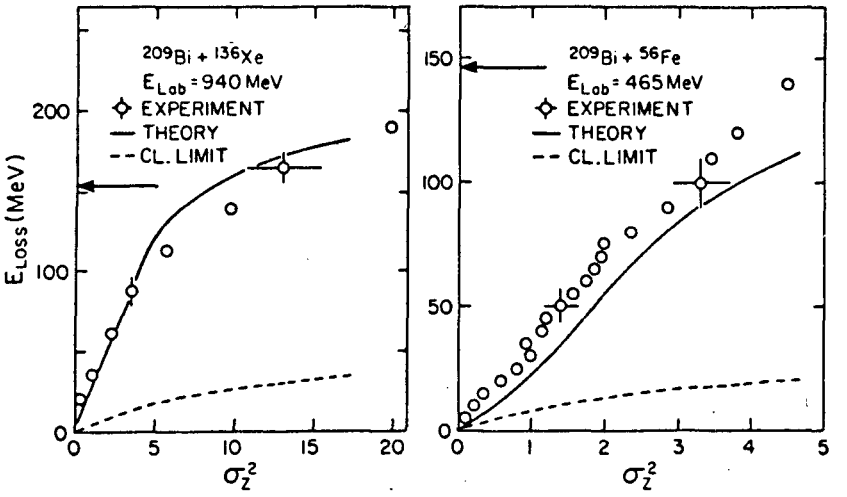

Fig. 7. Correlation between energy loss and charge variance for two reactions.[18] The dashed line and the solid line correspond to calculations without and with the Pauli principle, respectively, in terms of a one-body theory.

The particle transfer process deposits the same energy in both fragments when the two one-way fluxes are the same. If the system is asymmetric, the smaller fragment must then grow hotter because of its smaller heat capacity. The temperature gradient that ensues creates an imbalance in the particle fluxes, the large fragment receiving more particles than it gives away. The energy deposition on each fragment is proportional to the number of nucleons that land on it. Therefore, more energy will now be deposited on the heavy fragment, and this will tend to correct the temperature gradient. In other words, we are observing a feedback effect that leads to a self-regulation in the energy partition. In different words, the initially generated thermal imbalance redirects the energy deposition towards the larger fragment and controls the thermal gradient, but at the expense of the light fragment mass![19]

This explanation is particularly satisfactory because: a) the energy thermalization does not arise from the heat conductivity, which is in fact quite small, but from the fast redirection of the energy being dissipated; b) it creates a drive towards increasing asymmetry that may resist an opposite conservative force; and c) these effects rely on the presence of energy in the relative motion and disappear rapidly after the two fragments are at rest.

A calculation[19] performed for an asymmetric system (A_1 = 50, A_2 = 150) at 300 MeV center-of-mass energy is shown in fig. 8 for the following values of μ - B (where μ is the chemical potential and B the barrier between the two wells): 0.5 MeV, 10 MeV, 20 MeV, 30 MeV, and 40 MeV. The temperature dependence of the one-sided flux goes from very great at the lower range of this interval to minimal at the upper range. The upper part of fig. 8 shows the temperature ratio T_1/T_2 as a function of kinetic energy. For very low barriers (e.g., μ - B = 40 MeV) the temperature ratio goes rapidly up to $\sqrt{3}$ consistently with equal energy deposition and weakly declines thereafter. The effect of thermal conductivity is visible in the very late decline associated with the largest energy losses. In this regime there is little

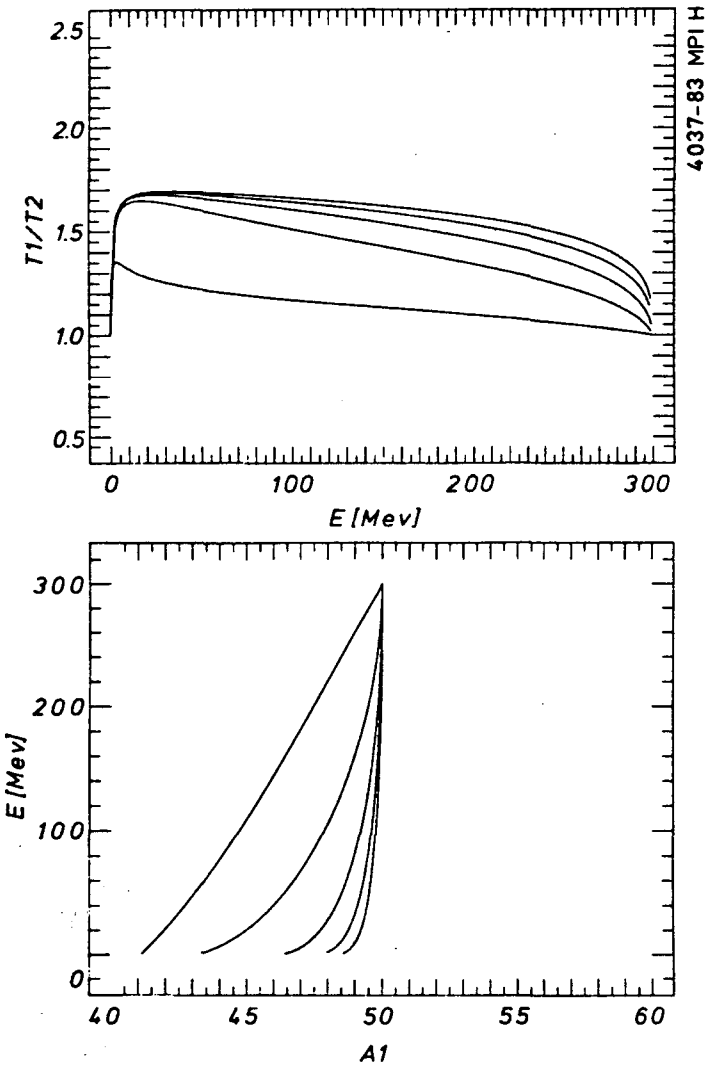

XBL 838-10939

Fig. 8.
Top: Temperature ratio vs total kinetic energy loss for a set of values of μ - B (see text), from bottom to top.
Bottom: Light fragment mass vs kinetic energy for the same values of μ - B from right to left.[19]

self-regulation and a very slow thermalization. For a barrier very close to the Fermi surface the result is dramatically different. The initial rise in temperature ratio is quickly controlled by the feedback effect and kept within a narrow range above unity throughout the Q-value range. In this case we see that the feedback effect is present and that it leads to a very nearly thermalized energy partition even at moderately low energy losses.

The lower part of Fig. 8 shows the dependence of the mass of the light fragment on energy loss. For low barrier values the mass remains fixed near 50 for most of the Q-value range. Only very late in the collision does one observe a decrease in mass as a late and slow response of the system to a great temperature gradient. For barriers near the Fermi surface the fluxes become substantially imbalanced at once, and the light fragment loses mass steadily throughout the Q-value range. This calculation quantitatively verifies our expectation. When the barrier is close to the Fermi surface, the temperature dependence of the fluxes is sufficiently strong to set a strong feedback effect in motion leading to a fine control of the temperature gradient on one hand and to a steady mass loss suffered by the light fragment on the other.

In fig. 9 the effect of a progressively greater driving force towards symmetry is studied. The curves shown represent the light fragment mass as a function of kinetic energy for the following

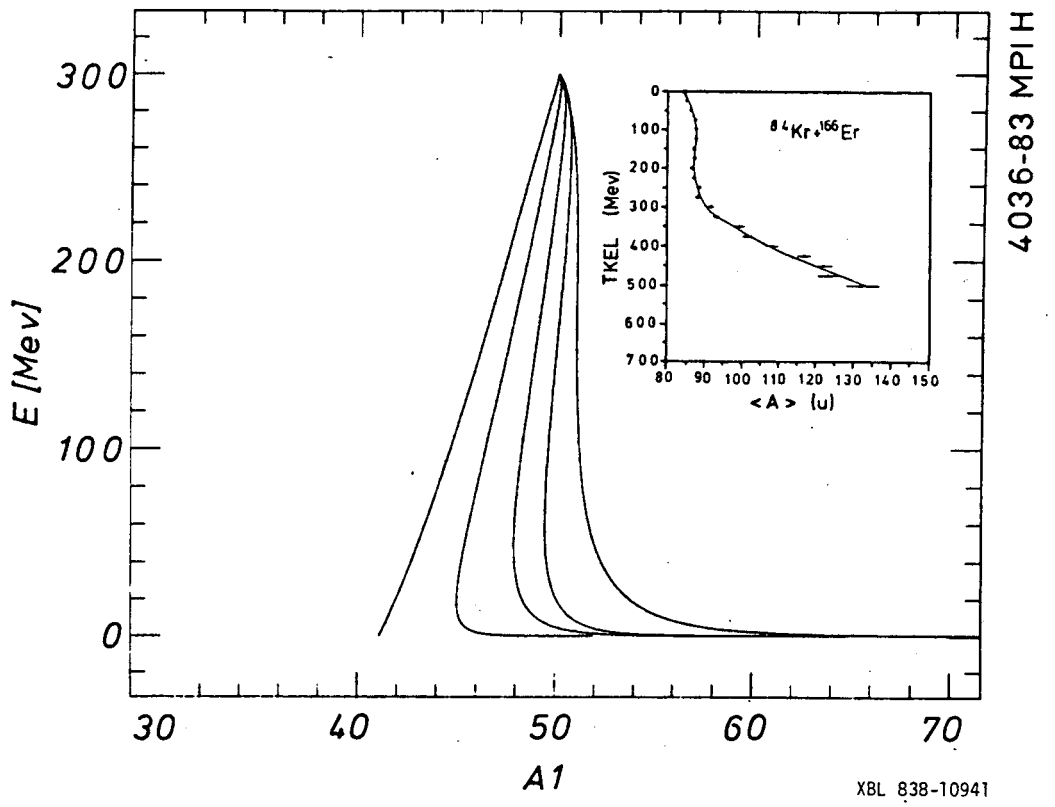

Fig. 9. Light fragment mass vs kinetic energy for increasing driving forces (see text)(left to right).[19] The inset shows the experimental pre-evaporation mass in the reaction ^{84}Kr + ^{166}Er.[20]

driving forces: 0, 0.5, 1.0, 1.5, 2.0 MeV/A, the lower Fermi surface being 0.5 MeV above the barrier. For nonzero driving forces we observe an initial tendency of the system to move towards symmetry. This tendency is readily controlled and even inverted by the feedback process as soon as a temperature gradient is established. Only very late in the collision, when lack of energy in the relative motion prevents the feedback process from operating, can the system follow the driving force towards symmetry once again. As a whole, we see that the mass asymmetry can be readily stabilized near its initial value throughout the Q-value range, in agreement with experiment. The wiggly curve predicted by the theory suggests that a similar structure may be seen experimentally. In the inset of fig. 9 the pre-evaporation light fragment mass vs Q-value for the reaction Kr + Er[20] shows a behavior that is not unlike that predicted by this theory.

The response of the system to a driving force depends rather strongly on the difference between average chemical potential and the barrier μ - B. Large values of μ - B lead to a small mass drift when observed against energy loss. The relation between energy loss and light fragment mass is shown in fig. 10 for μ - B = 50, 10, 0.5 MeV with a driving force of 1.5 MeV. The systematic increase of the mobility with decreasing μ - B is readily seen at small energy losses. However, at the smallest values of μ - B the increased mobility is compensated by the feedback effect, which, as was already seen in fig. 9, stabilizes the mass near the entrance channel value. Consequently, while a small mass drift could be consistent with either large or small μ - B, the near

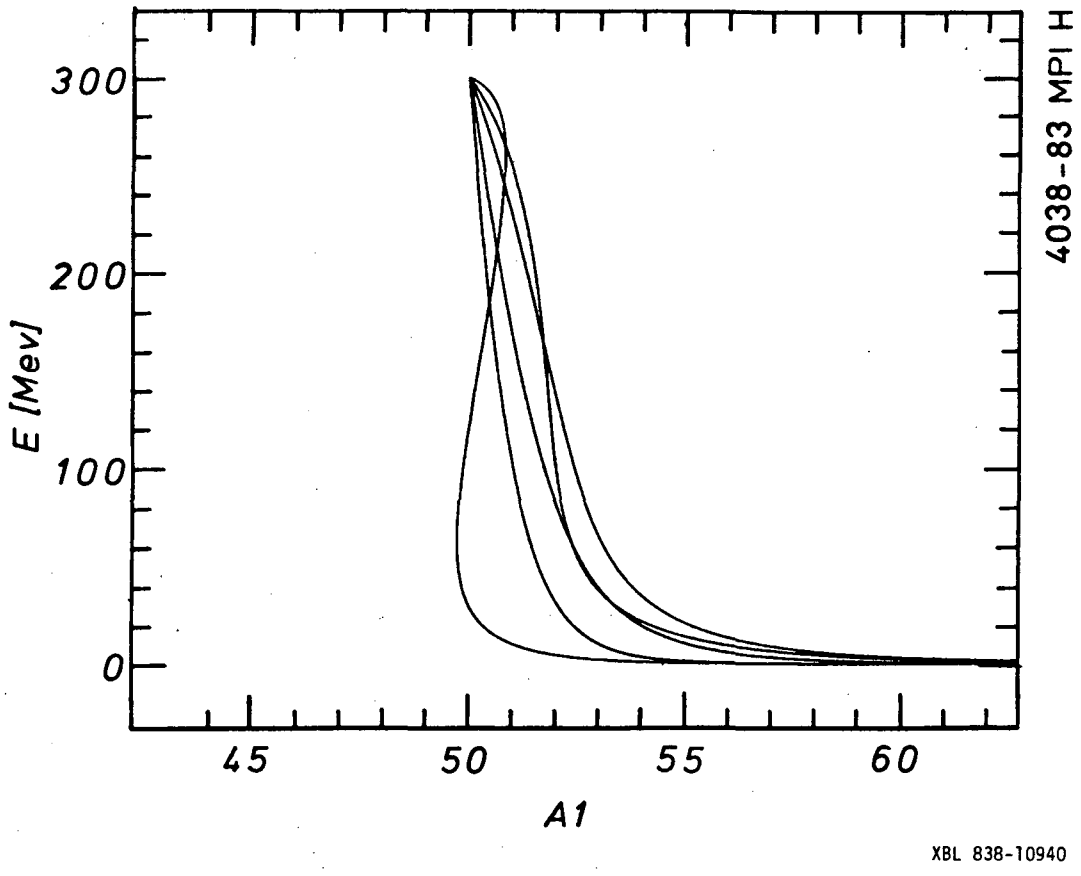

Fig. 10. Light fragment mass vs kinetic energy for different values of $\mu - B$ and a fixed driving force.[19]

thermalization of the dissipated energy is consistent only with a small value of $\mu - B$.

c) The distribution in the neutron-to-proton ratio

Two nuclei with masses A_1, A_2 and charges Z_1, Z_2 are allowed to come into contact. Assuming that the masses cannot be altered but only the charges, what is the expected equilibrium distribution in charge? Let us write down the potential energy of the system as a function of the charge of one of the fragments:

$$V(Z_1) = E_{LD}\,(Z_1, A_1) + E_{LD}\,(Z_2, A_2) + \frac{Z_1 Z_2 e^2}{R_1 + R_2} \tag{8}$$

The most probable charge at fixed mass is given by

$$\left.\frac{\partial V(Z_1)}{\partial Z_1}\right|_{A_1} = 0 \tag{9}$$

This result predicts that the collision between a (neutron-rich) heavy nucleus and a (neutron-poor) light nucleus should produce neutron-rich light fragments. This result has been amply verified experimentally, and this kind of reaction has been used to produce some new neutron-rich light nuclei. The thermal distribution can be immediately derived. Eq. (9) can be rewritten as

$$V \cong \frac{1}{2} c \, (Z - \hat{Z})^2 \tag{10}$$

and the classical thermal distribution is

$$P(Z_1) \propto \exp - \frac{C(Z_1 - \hat{Z}_1)}{2T} \tag{11}$$

or a Gaussian with variance $\sigma^2 = \frac{T}{C}$

Some experimental data[21] seem to confirm such a prediction as shown in fig. 11. The classical result of eq. (11) holds also in the quantum case if $T \gg \hbar\omega$. Otherwise one should have

$$P(Z_1) = \left(\frac{\omega}{\pi\hbar} \tanh \frac{\hbar\omega}{2T}\right)^{1/2} \exp \left\{ -q^2 \frac{\omega}{\hbar} \tanh \frac{\hbar\omega}{2T} \right\} \tag{12}$$

where $q = Z_1 - \hat{Z}_1$. In the limit $\hbar\omega \gg T$ one obtains the simple result

$$\sigma^2 = \frac{\hbar\omega}{2C} \tag{13}$$

If the mode we are considering can be identified with the giant E1 vibration of a very deformed nucleus along its major axis we may expect

$$\hbar\omega \approx 94/d \text{ MeV} \tag{14}$$

where d is the semimajor axis of the dinuclear system in Fermi. Under these circumstances the limit of eq. (13) should prevail, and a variance nearly independent of excitation energy should be expected. This seems to be reflected in some experimental data[22] shown in fig. 12. From a theoretical standpoint there are several difficulties associated with this quantal result. For instance, it is doubtful that the phonon energy can be obtained in such a trivial generalization as in eq. (14) since the role of the neck constriction in the dinuclear shape should be very important in increasing the inertia and thus in decreasing the phonon energy. Furthermore, more than one multipole may be playing an important role, and the various multipoles may contribute in a different way depending on the mass asymmetry.[23] Finally, a strong damping may spread the mode(s) so much that no characteristic frequency can be associated with it, in which case eq. (11) would be again the correct limit.

d) <u>The partition of angular momentum</u>

Two nuclei in contact can carry angular momentum both in the form of intrinsic spin and in the form of orbital motion. For two equal spheres in contact it is easy to identify the angular-momentum-bearing normal modes. Their traditional names that arose in dealing with an analogous problem in fission are: two bending modes, one twisting mode, two wriggling modes, and one tilting mode.

The statistical mechanics of such a system is quite simple.[24] In particular, the distribution of the three angular-momentum components of each of the two equal nuclei is a Gaussian:

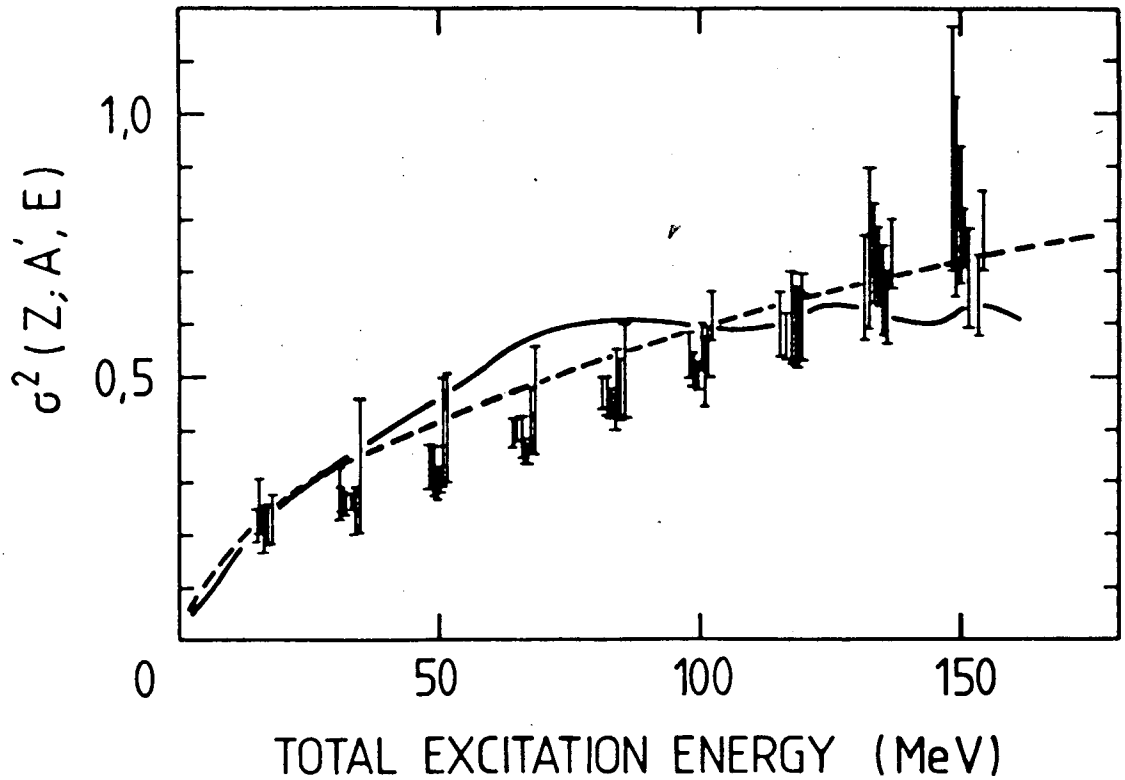

Fig. 11. Isobaric charge distribution variances as a function of excitation energy for the system $^{132}Xe + ^{197}Au$.[21]

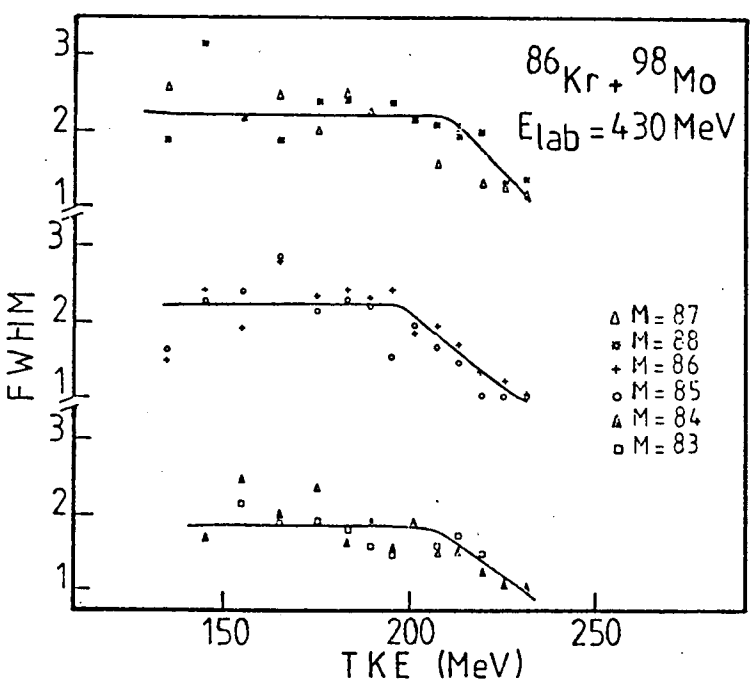

Fig. 12. Width of the isobaric charge distribution as a function of exit channel kinetic energy.[22]

$$P(I_x,I_y,I_z) \propto \exp - \left\{ \frac{I_x^2}{2\sigma_x^2} + \frac{I_y^2}{2\sigma_y^2} + \frac{(I_z-\langle I_z\rangle)^2}{2\sigma_z^2} \right\} \tag{15}$$

The y-axis is chosen to be the symmetry axis and the z-axis is chosen parallel to the total angular momentum. The average z-component $\langle I_z\rangle$ is the expected contribution to the spin of one fragment from rigid rotation. In this particular case, it amounts to one-seventh of the total angular momentum. The variances can be expressed in terms of the temperature T and of the moment of inertia $\mathcal{J}$ of one of the two fragments.

$$\sigma_x^2 = \frac{6}{5}\mathcal{J}T; \quad \sigma_y^2 = \frac{6}{7}\mathcal{J}T; \quad \sigma_z^2 = \frac{6}{7}\mathcal{J}T \tag{16}$$

The formalism can be easily generalized for shapes different from spheres and for asymmetric systems.[25] At zero temperature we recover the secular equilibrium result of rigid rotation. At temperatures larger than zero, the thermal fluctuations become important. Their effect should be particularly visible in the misalignment of the fragments' spins.

The limit of rigid rotation has been verified in two ways. One method uses the gamma-ray multiplicity associated with a heavy-ion collision to infer the sum of the moduli of the fragments' spins. When the measurement is performed as a function of the exit-channel mass asymmetry, one should observe a rise of the multiplicity and thus of the sum of the fragments' spins with increasing asymmetry. This has been observed in some reactions like Ne + Ag[26], Ar + Y[27], and Ag + Ar where deep-inelastic processes are confined to a narrow ℓ-wave window (fig. 13). In

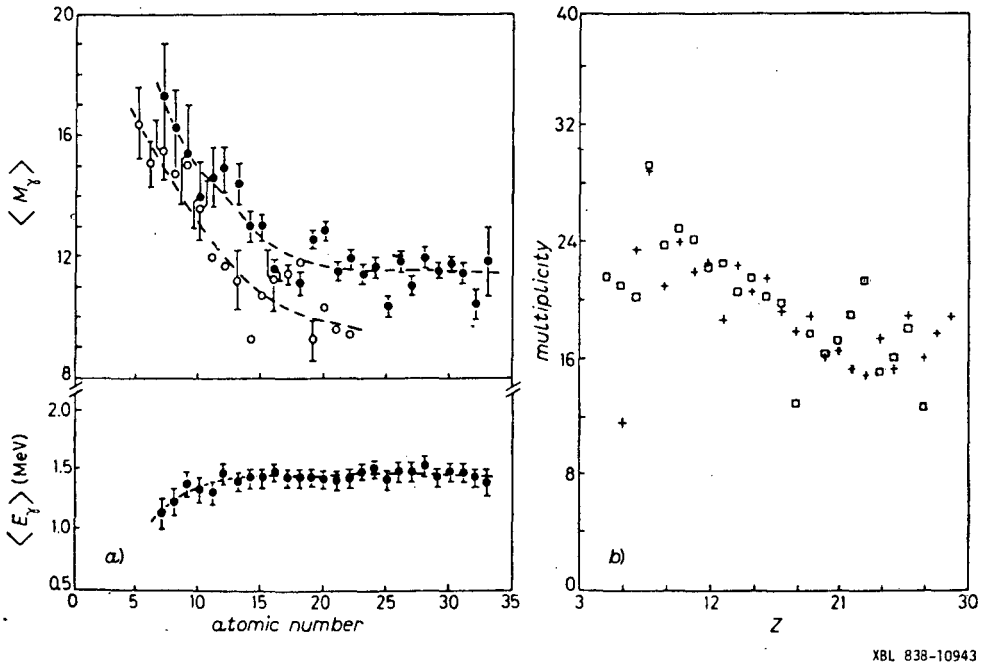

Fig. 13. a) Gamma-ray multiplicities vs atomic number for the reactions 175 MeV ^{20}Ne + Ag at 90° (lab)[26] (o) and for the reaction 237 MeV ^{40}Ar + ^{89}Y (•).[27] In the lower part of the figure the average gamma-ray energies for the latter reaction are also given.[27] b) Gamma-ray multiplicity vs atomic number for the reaction ^{107,109}Ag + 288 MeV ^{40}Ar (crosses) and ^{107,109}Ag + 340 MeV ^{40}Ar (open squares) (author's unpublished data).

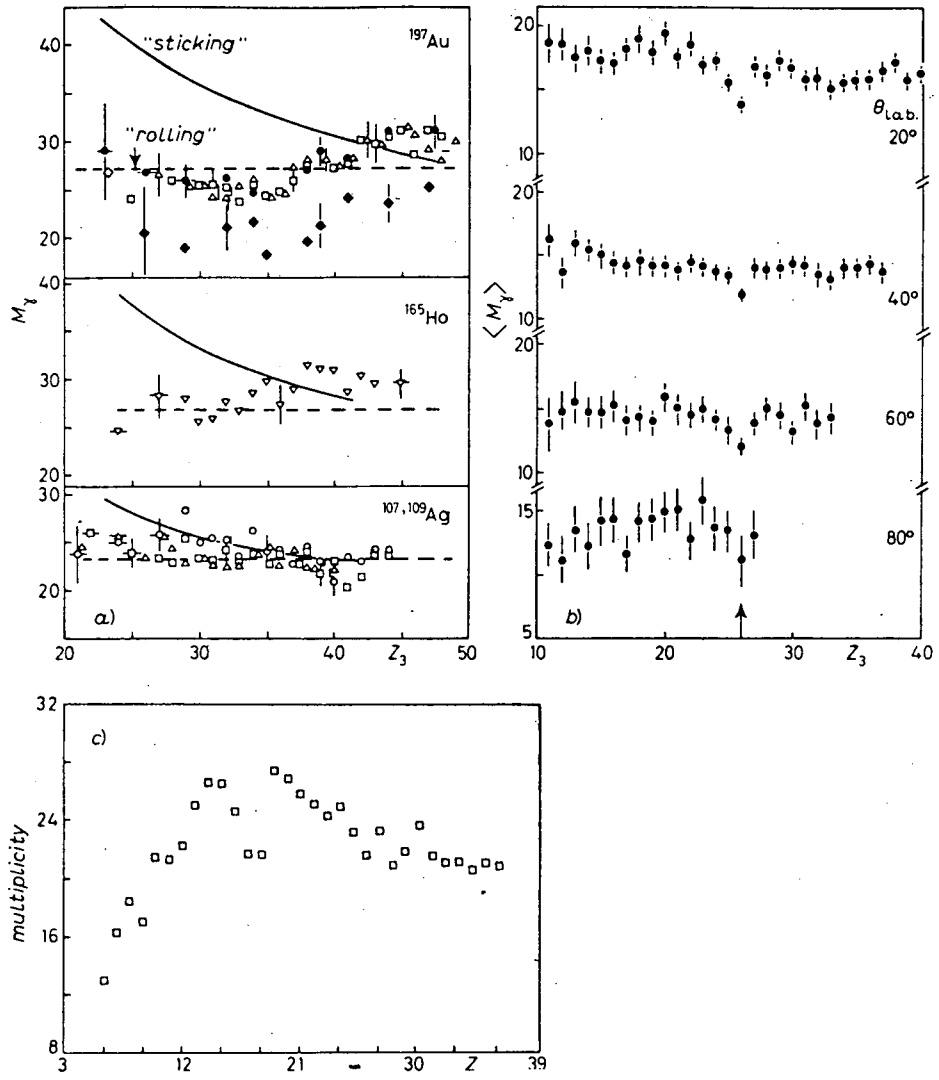

XBL 838-10944

Fig. 14. a) Gamma-ray multiplicities vs Z for the deep inelastic component in 618 MeV ^{86}Kr + $^{107,109}Ag$, ^{165}Ho and ^{197}Au:[28] ○ 20°, □ 30°, ▼ 35°, △ 40°, ● 55°, ◆ 70°. b) Same as in a) for the reaction 470 MeV ^{56}Fe + $^{107,109}Ag$ (author's unpublished data). Notice the angular dependence of M_γ. c) Same as in a) for the reaction 340 MeV ^{40}Ar + Tb (author's unpublished data). Notice the precipitous drop of M_γ at low Z's.

reactions like Kr + heavy targets,[28] where a large ℓ-window is involved, a flat dependence of the gamma-ray multiplicity on mass asymmetry is interpreted as due to rigid rotation associated with angular-momentum fractionation along the mass asymmetry coordinate. This is shown in fig. 14. In other words, the high ℓ-waves remain confined near the entrance-channel mass asymmetry while the lower ℓ-waves spread more and more away from the entrance-channel mass asymmetry. An intermediate and more complex situation is shown in fig. 14c.

A second and more powerful method involves the determination of the spin of an individual fragment from the out-of-plane angular distribution of the sequentially emitted alpha particles. The results from such an experiment on the reaction Kr + Ag[29] are given in fig. 15. In this figure the spin of the heavy fragment (full circles) is plotted as a function of the atomic number of the light fragment in coincidence. The rapid rise of the spin with increasing asymmetry as well as the comparison with a calculation (lower line) indicate the presence of rigid rotation. The open circles represent the sum of the spins obtained from a gamma-ray multiplicity measurement in the same experiment, while the solid squares represent the sum of the spins inferred from the heavy fragment spin. The comparison between the open circles and the solid squares indicates the high reliability of the two methods. One can conclude that rigid rotation is indeed attained in the studies illustrated above, and that it prevails in the Q-value region corresponding to complete relaxation of the kinetic energy.

As we have mentioned above, the presence of in-plane fluctuating components must lead to a misalignment of the fragments' spins. We have performed a particularly thorough study of the angular-momentum transfer and misalignment by measuring the gamma-ray multiplicity and angular distribution as a function of Q-value for a series of reactions. We report here the results obtained for the reactions 1400 MeV ^{165}Ho + (^{176}Yb, ^{148}Sm, ^{nat}Ag).[30]

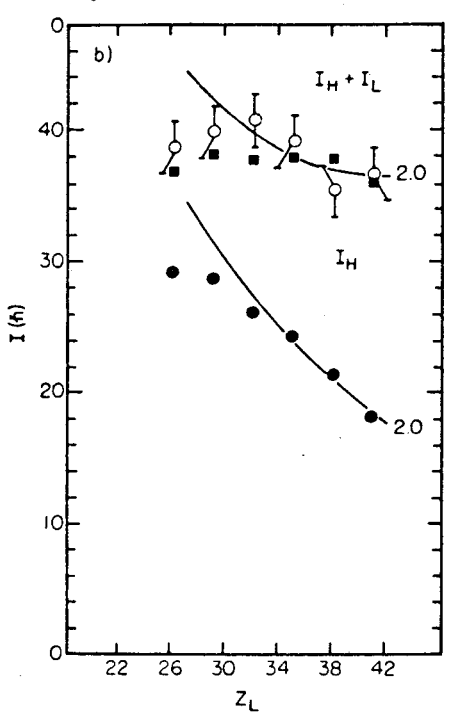

Fig. 15. Spin of the heavy fragment as a function of the atomic number of the coincident fragment determined from alpha particle angular distributions (dots). The sum of the spins inferred from the previous measurement is also shown (squares) as well as that determined from γ-ray multiplicities (open circles). The lines correspond to the rigid rotation limit for two touching spheroids with the ratio of axes equal to 2:1.[29]

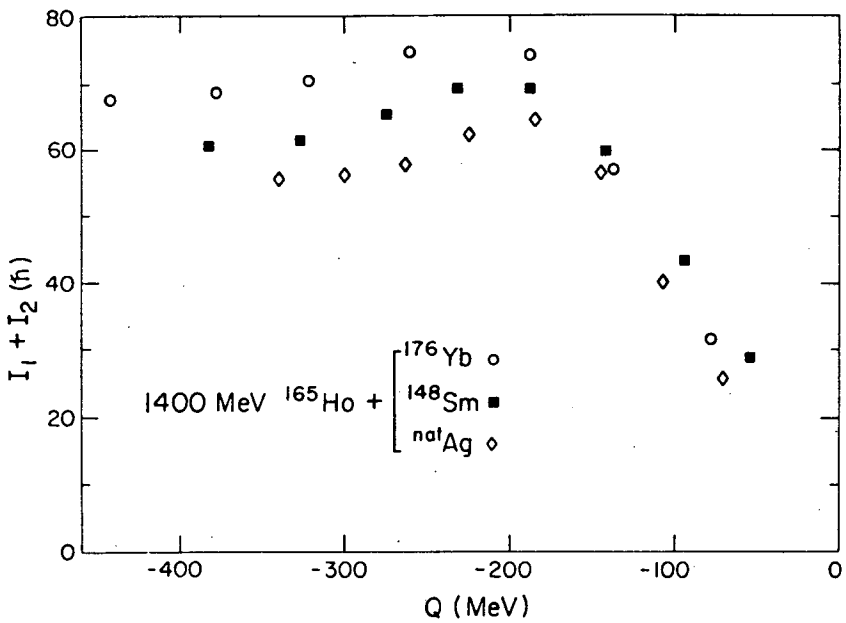

Fig. 16. Sum of the fragments spins vs Q-value for three reactions.[30)]

Figure 16 shows the sum of the fragments' spins as a function of Q-value for the three reactions as inferred from the gamma-ray multiplicities. We observe an initially rapid increase of the spin with increasing negative Q-value, due to the relaxation towards rigid rotation. Eventually, the spins saturate and actually tend to decrease with increasing negative Q-value, as rigid rotation is attained and progressively lower ℓ-waves are sampled. The prevalence of rigid rotation can be seen in fig. 17. In the upper part a scaling based on the rolling limit is used, while in the lower part the scaling assumes rigid rotation. The abscissa is scaled in terms of the nuclear temperature. It can be seen that under the assumption of rigid rotation one obtains an essentially perfect scaling for the three reactions.

The in-plane/out-of-plane anisotropy of the stretched quadrupole component of the gamma-ray spectrum should be infinite if one has perfect alignment, following the expected angular distribution pattern $\omega(\theta) = \frac{5}{4}(1 - \cos^4\theta)$ where θ is the angle between the spin vector and the gamma-ray direction. The anisotropy is rapidly reduced if the spin is misaligned by the presence of in-plane fluctuating components. Of course, in real life one has to worry about the presence of stretched and nonstretched E1 components and about a secondary misalignment arising from particle evaporation. In fig. 18 the gamma-ray anisotropies are shown as a function of Q-value for the three reactions. In all the three cases, the anisotropy rises sharply with increasing negative Q-value, reaches a maximum where the gamma-ray multiplicity begins to saturate, and falls beyond that point until isotropy is reached once again.

A qualitative understanding of this rise and fall of the anisotropy can be easily reached. At the very lowest Q-values the angular momentum fed to the fragments is so small that it is easily misaligned by any tiny in-plane component. As the energy dissipation increases, spin is rapidly fed to the fragments while the fluctuations increase very slowly (remember $\sigma^2_{x,y,x} \approx \mathcal{J}T$, so $\sigma_{x,y,x}$ increases with the fourth root of the Q-value) and the system becomes more and more aligned. Beyond the maximum of the anisotropy, the z-component of the fragment spin actually

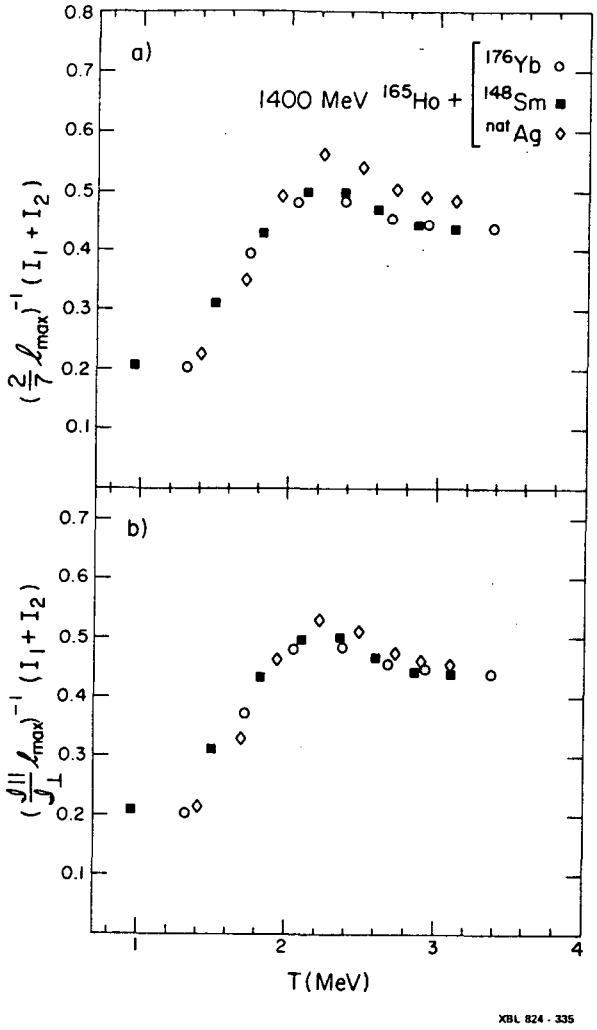

Fig. 17. The sum of spins in reduced units as a function of temperature. The angular momentum axes have been scaled according to the "rolling" limit for part (a) and to rigid-rotation limit for part (b).[30]

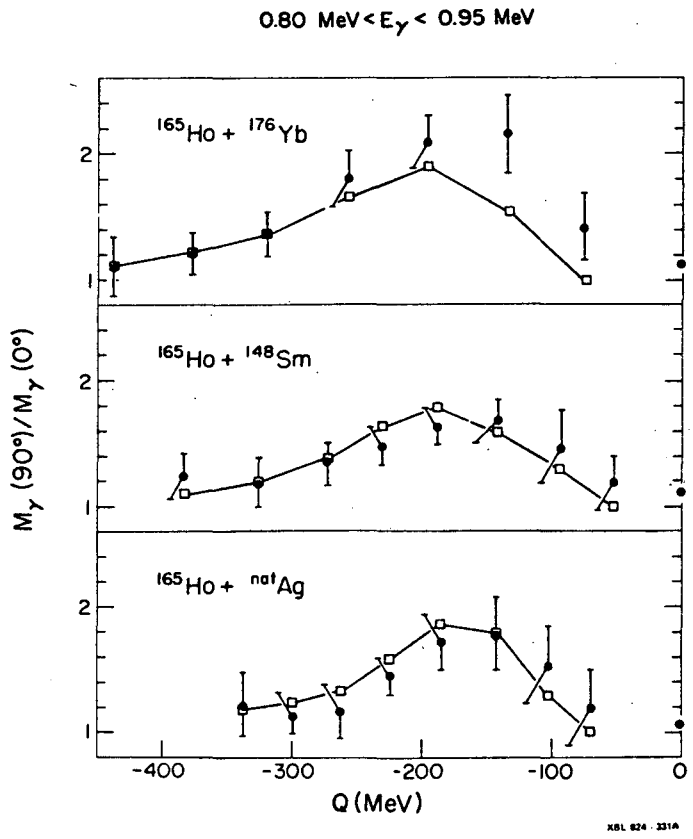

Fig. 18. Gamma-ray anisotropies vs Q-value for three reactions. The open squares connected with a line represent a calculation based on the statistical model for the angular momentum misalignment.[30]

decreases, while the fluctuations keep increasing. As a consequence, the spin becomes seriously misaligned and the anisotropy falls. The squares connected by lines in fig. 18 represent a calculation where the theory [eq. (15,16)] provides the fluctuations and the experiment, in a self-consistent way, provides the average z-component. Corrections for the presence of E1 components, for the misalignment associated with particle evaporation, etc. have been incorporated. The agreement with the data shows that, even in the region of incomplete angular-momentum relaxation, the fluctuations calculated in terms of a thermal model give an adequate explanation of the data. The success of an equilibrium model in evaluating the fluctuations in an obvious nonequilibrium regime is not surprising, as the fluctuations reach within a few percent of the equilibrium value in a fraction of relaxation time. The primary spin misalignment associated with each fragment can be obtained if one assumes that the angular momenta are partitioned according to rigid rotation as suggested by fig. 17. The diagonal component of the polarization tensor, $P_{zz} = \frac{3}{2}\frac{\langle I_z^2\rangle}{\langle I^2\rangle} - \frac{1}{2}$ for each fragment is shown in fig. 19. It is interesting to notice that in an asymmetric system it is the light fragment that becomes more misaligned.

e) Angular distributions: quantal and statistical fluctuations

In the statistical limit of full relaxation and long interaction times, the angular distribution of the fragments should be similar to that of an equivalent fissioning system, namely symmetric about 90° in the center of mass and approaching $1/\sin\theta$ for large angular momenta.

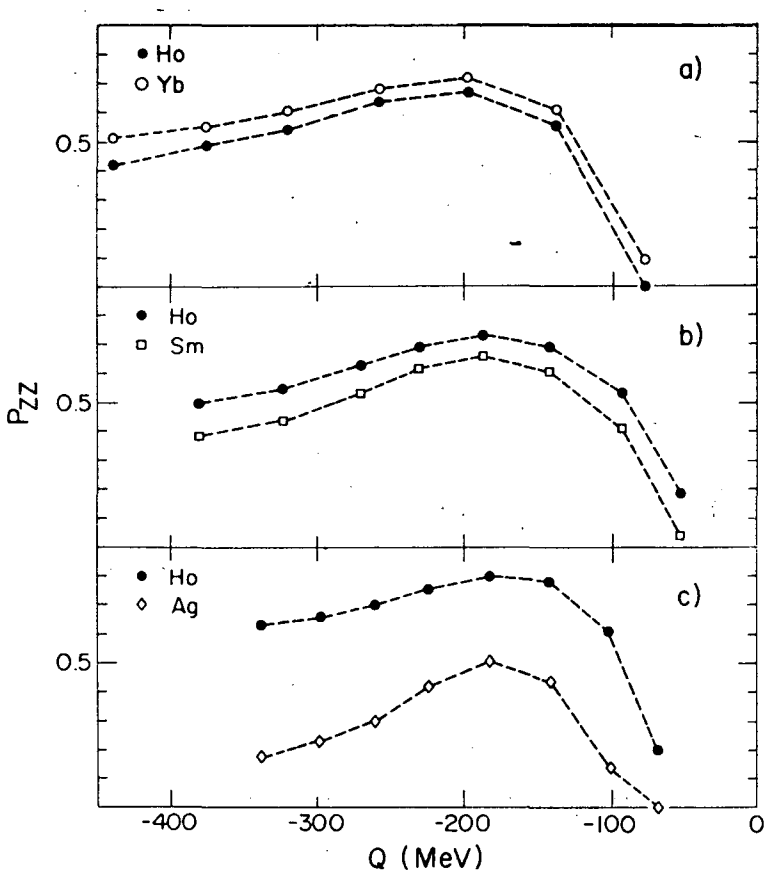

Fig. 19. Alignment parameter P_{zz} as a function of Q-value, for each of the two deep-inelastic fragments in the three reactions.

Experimentally, the angular distributions observed in deep inelastic processes vary from side-peaked to forward-peaked, frequently in the same reactions. The side-peaking is found at relatively low Q-values and near the entrance-channel mass asymmetry, while the forward-peaking is apparent with increasing inelasticity and for mass asymmetries far from that of the entrance channel.[2] Such a remarkable evolution must find its counterpart in a great variation in the interaction time on one hand, and in a rapid change in the width of the orbital angular momentum distribution on the other.

When a side-peaked angular distribution is present, it can be parameterized in terms of a center angle $\hat{\theta}$ and of its width σ_θ. What information can be obtained from these two quantities? The center angle $\hat{\theta}$ can be of use in constructing the deflection function if it can be associated with some average angular momentum. This can be tried by assuming a monotonic dependence[2,31] of the energy on angular momentum and by finding the l-space bin corresponding to the energy bin under consideration by means of the associated cross section. The width of the distribution arises from two contributions, as pointed out by Strutinski,[32] namely a "diffractive" contribution, associated with the width of the l-packet, and a "dynamical" contribution associated with the classical deflection function. More precisely:

$$\sigma_\theta^2 = \frac{1}{4\sigma_l^2} + \left(\frac{d\theta}{dl}\right)^2 \sigma_l^2 \tag{17}$$

The first term can be readily derived from the indetermination principle, while the second propagates the width of the l-packet in angle through the deflection function $\theta = \theta(l)$. An interesting application of the above equation is in providing a simple explanation to some complex calculations. A Wilczinski diagram generated with a diffusion calculation[33] is unable to reproduce the width of the angular distribution at small energy losses as shown in fig. 20a. This is due to the fact that the fluctuations in l depend on the temperature, namely, $\sigma_l^2 \propto T$. The introduction of quantal fluctuations results in a greatly broadened and more realistic diagram as illustrated in fig. 20b. The quantal broadening is, of course, arising from the narrow thermal l-distribution. On the other hand, a Wilczinski diagram generated with a one-body diffusion model (fig. 21) is quite realistic even at small Q-values without quantal fluctuations. In fact, the introduction of quantal fluctuations does not broaden the angular distributions appreciably.[34] The explanation lies in the fact that the one-body theory predicts a large "dynamical" σ_l even for low Q-values, which is, of course, responsible for the broad angular distributions. But a <u>large</u> σ_l implies a <u>small</u> quantal fluctuation. Therefore, the introduction of quantal fluctuations hardly changes the results. This illustrates how from true experimental data one can extract σ_l and compare it directly with theoretical predictions. Of course, one trivial component of σ_l is due to the energy binning or

$$\sigma_l^2 = \left(\frac{dl}{dE}\right)^2 \sigma_E^2 \quad . \tag{18}$$

The remainder of the width arises from true orbital angular momentum fluctuations.

An obvious source of l-fluctuations is the coupling with a "wriggling" mode.[24] In this coupling, orbital angular momentum can be traded for spin and vice versa. The thermal limit is easy to calculate, especially for two touching spheres.[35]

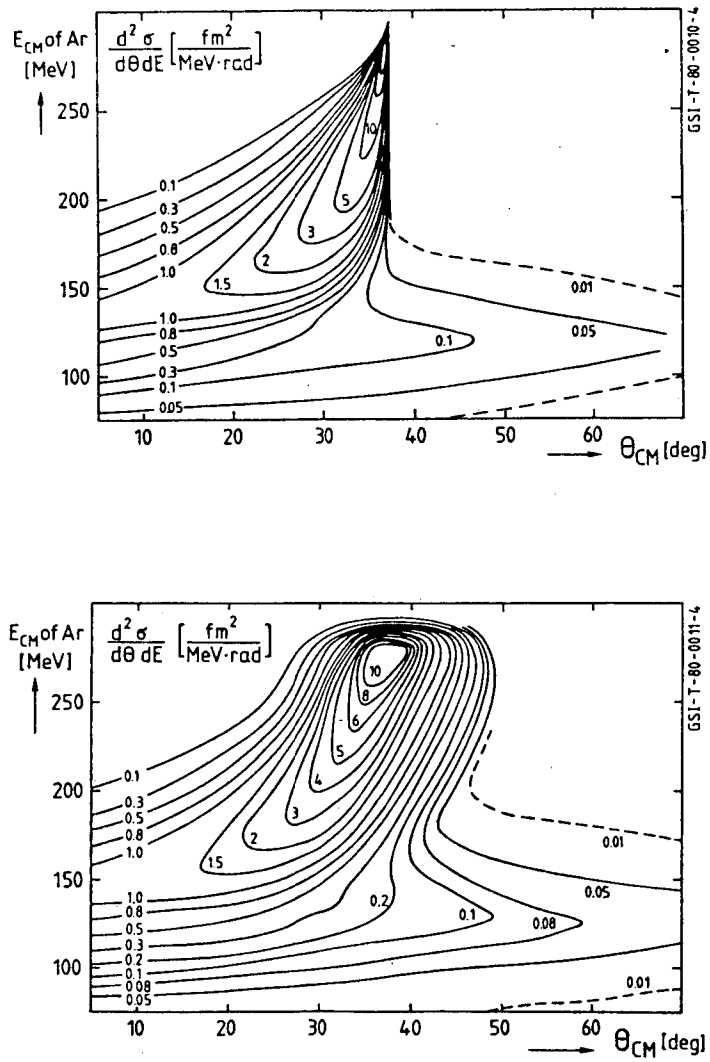

Fig. 20. Wilczynski plot calculated without (top) and with (bottom) quantal fluctuations.[33]

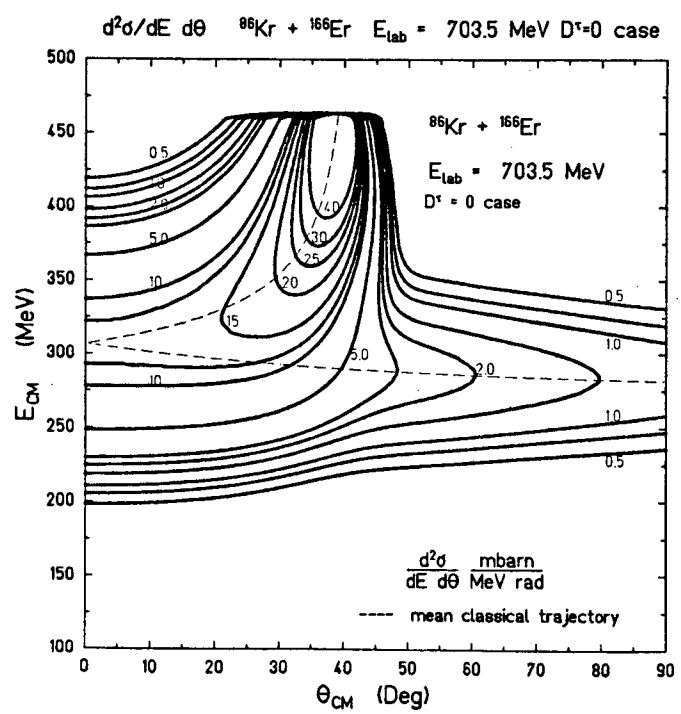

Fig. 21. Wilczynski plot calculated from a one-body theory and without quantal fluctuations.[34]

If I is the total angular momentum, the total rotational energy is

$$E_R = \frac{l^2}{2\mathcal{J}^*} + \frac{I^2}{4\mathcal{J}} - \frac{Il}{2\mathcal{J}} \text{ where } \frac{1}{\mathcal{J}^*} = \frac{1}{\mu R^2} + \frac{1}{2\mathcal{J}}$$

and $\mathcal{J}$ is the moment of inertia of one of the spheres. The orbital angular momentum distribution at fixed I is

$$P(l)dl = (2\pi\mathcal{J}T)^{-1/2} \exp -\left(\frac{l^2}{2\mathcal{J}^*T} - \frac{Il}{2\mathcal{J}T} + I^2 \frac{\mathcal{J}^*}{8\mathcal{J}^2T}\right)$$

Introducing a 2IdI weight, remembering that the exit channel kinetic energy above the Coulomb energy is $E = l^2/2\mu R^2$ and introducing the reduced variables $\varepsilon = E/T$, $\lambda = I/(\mathcal{J}T)^{1/2}$, one obtains

$$P(\varepsilon,\lambda) \propto \frac{\lambda}{\varepsilon} \exp - \left[\frac{7}{2}\varepsilon - \frac{5}{2}\lambda\varepsilon + \frac{5}{28}\lambda^2\right]$$

At constant energy ε the most probable value of the angular momentum is

$$\lambda = \frac{7}{\sqrt{10}}\sqrt{\varepsilon}\left(1 + \quad 1 + \sqrt{\frac{4}{7\varepsilon}}\right)$$

while the variance, in which we are mainly interested, is

$$\sigma_\lambda^2 = \frac{14}{5} \text{ or } \sigma_l^2 = \frac{14}{5}\mathcal{J}T \quad .$$

A further source of l-fluctuations is due to shape fluctuations in the dinucleus.[35] Calculations in the thermal limit show that very substantial fluctuations in orbital angular momentum can be expected at fixed energy if shape fluctuations should occur.

In both cases considered above, we have an interesting correlation: the leading edge of the angular distribution corresponds to $l > \hat{l}$ while the trailing edge corresponds to $l < \hat{l}$. This discussion suggests some possible experimental tests. For instance, the fluctuations in l measured from the angular distribution widths should find their counterpart in the spin fluctuations in the same energy bin. The spin fluctuations can be obtained, for instance, from a measurement of the spin misalignment.

Perhaps even more interestingly, one could measure the spins (e.g., gamma-ray multiplicities) to the left and to the right of the angular distribution peak and verify that the gamma multiplicity to the right is greater than the gamma multiplicity to the left.

Conclusion

Perhaps it is worth trying to write two conclusions rather than one. The first deals with the deep-inelastic processes and the second with the statistical approach. Deep-inelastic processes have succeeded in creating or at least in enhancing the awareness that nuclei are not only spherical or slightly deformed, but can exist, at least temporarily, in extremely peculiar shapes and in conditions far removed from equilibrium. The associated problems of energy dissipation, mass transfer, and charge equilibration have kept many of us busy for the last few years and have created a lexicon that now is an integral part of the language of a nuclear physicist.

The statistical approach has shown that a "conditional equilibrium" prevails for many degrees of freedom and that an equilibrium or a nonequilibrium statistical treatment is, at least phenomenologically, able to account for most of the experimental data. At the very least the statistical approach has given us a

solid reference, an effective pedagogical guide, and not a small number of explanations.

This work was supported by the Director, Office of Energy Research, Division of Nuclear Physics of the Office of High Energy and Nuclear Physics of the U.S. Department of Energy under Contract DE-AC03-76SF00098.

References

1) A readable overview of this subject is given by: Ilya Prigogine "From Being to Becoming. Time and Complexity in the Physical Sciences," W.H. Freeman and Company, San Francisco; while a formal presentation is given in: A.J. Lichtenberg and M.A. Lieberman. Regular and Stochastic Motion, Springer-Verglag, New York, Heidelberg, Berlin.
2) The interested reader can benefit from the following review articles: W.U. Schröder, J.R. Huizenga, Ann. Rev. Nucl. Sci. 27 (1977) 465; M. Lefort and C. Ngo, Ann. Phys. (NY) 3 (1978) 5; L.G. Moretto and R.P. Schmitt, Rep. Prog. Phys. 44 (1981) 543.
3) L.G. Moretto and J.S. Sventek, Phys. Lett. 58B (1975) 26.
4) W. Nörenberg, Phys. Lett. 52B (1974) 289.
5) J. Randrup, Nucl. Phys. A307 (1978) 319; ibid A327 (1979) 490.
6) M. Dakowski, A. Gobbi, and W. Nörenberg, Nucl. Phys. A378 (1982) 189, and references therein.
7) W.J. Swiatecki, Nucl. Phys. A376 (1982) 275.
8) W. Nörenberg, Nucl. Phys. A400 (1983) 275c.
9) D.J. Morrissey and L.G. Moretto, Phys. Rev. C23 (1981) 1835.
10) B. Cauvin, R.C. Jared, P. Russo, R.P. Schmitt, R. Babinet, and L.G. Moretto, Nucl. Phys. A301 (1978) 511.
11) R. Babinet, B. Cauvin, J. Girard, H. Nifenecker, G. Gatty, D. Guerreau, M. Lefort, and X. Tarrago, Nucl. Phys. A296 (1978) 160.
12) B. Tamain, R. Chechik, H. Fuchs, F. Hanappe, M. Morjean, C. Ngô, J. Peter, Nucl. Phys. A330 (1979) 253.
13) Y. Eyal, A. Gavron, I. Tserruya, Z. Fraenkel, Y. Isen, S. Wald, R. Bass, J.R. Gould, G. Kreyling, R. Renfordt, K. Stelzer, R. Zitzmann, A. Gobbi, U. Lynen, H. Stelzer, I. Rode, R. Bock, Phys. Rev. Lett. 41 (1978) 625.
14) D. Hilscher, J.R. Birkelund, A.D. Hoover, W.U. Schröder, W.W. Wilke, J.R. Huizenga, A. Mignerey, K.C. Wolf, H.F. Breuer, V.I. Viola, Phys. Rev. C20 (1979) 576.
15) R.P. Schmitt, G.J. Wozniak, G.U. Rattazzi, G. Mathews, R. Regimbart, and L.G. Moretto, Phys. Rev. Lett. 46 (1981) 522.
16) G. Rudolf, A. Gobbi, H. Stelzer, U. Lynen, A. Olmi, N. Sann, R.G. Stokstad, and D. Pelte, Nucl. Phys. A330 (1979) 245.
17) L.G. Moretto and J.S. Sventek, Proceedings of the Symposium on Macroscopic Features of Heavy Ion Collisions, 1 (1976) 235, Argonne National Report ANL/PHY-76-2.
18) W.U. Schröder, J.R. Birkelund, J.R. Huizenga, W.W. Wilcke, and J. Randrup, Phys. Rev. Lett. 44 (1980) 300.
19) L.G. Moretto and E.G. Lanza, Lawrence Berkeley Laboratory Preprint 16373 (1983).
20) P. Glassel, D.v. Harrach, L. Grodzins, H.J. Specht, Z. Phys. A310 (1983) 189.
21) J.V. Kratz, J. Poitou, W. Bruchle, H. Gaggeler, M. Schadel, G. Wirth, and R. Lucas, Nucl. Phys. A357 (1981) 437.

22) M. Berlanger, A. Gobbi, F. Hanappe, U. Lynen, C. Ngô, A. Olmi, H. Sann, H. Stelzer, H. Richel, and M.F. Rivet, Z. Phys. A291 (1979) 133.
23) L.G. Moretto, C.R. Albiston, and G. Mantzouranis, Phys. Rev. Lett. 44 (1980) 924.
24) L.G. Moretto and R.P. Schmitt, Phys. Rev. C21 (1980) 204.
25) R.P. Schmitt and A.J. Pacheco, Nucl. Phys. A379 (1982) 313.
26) P. Glassel, R.S. Simon, R.M. Diamond, R.C. Jared, I.Y. Lee, L.G. Moretto, J.O. Newton, R. Schmitt, and F. Stephens, Phys. Rev. Lett. 38 (1977) 331.
27) J.B. Natowitz, N.M. Namboodiri, P. Kasiraj, R. Eggers, L. Adler, P. Gontier, C. Cerutti, and T. Alleman, Phys. Rev. Lett. 40 (1978) 751.
28) M.M. Aleonard, G.J. Wozniak, P. Glassel, M.A. Deleplanque, R.M. Diamond, L.G. Moretto, R.P. Schmitt, and F.S. Stephens, Phys. Rev. Lett. 40 (1978) 622.
29) L.G. Sobotka, C.C. Hsu, G.J. Wozniak, D.J. Morrissey, and L.G. Moretto, Nucl. Phys. A371 (1981) 510.
30) A.J. Pacheco, G.J. Wozniak, R.J. McDonald, R.M. Diamond, C.C. Hsu, L.G. Moretto, D.J. Morrissey, L.C. Sobotka, and F.S. Stephens, Nucl. Phys. A397 (1983) 313.
31) W.V. Schröder, J.R. Birkelund, J.R. Huizenga, K.G. Wolf, and V.E. Viola, Jr., Phys. Rep. 45 (1978) 301.
32) V.H. Strutinski, Phys. Lett. 44B (1973) 245.
33) W. Cassing and H. Friedrich, Z. Phys. A298 (1980) 129.
34) H. Feldmeier, International School of Physics "Enrico Fermi" Varenna 1982.
35) L.G. Moretto and L.G. Sobotka, Z. Physik A303 (1981) 299.

This report was done with support from the Department of Energy. Any conclusions or opinions expressed in this report represent solely those of the author(s) and not necessarily those of The Regents of the University of California, the Lawrence Berkeley Laboratory or the Department of Energy.

Reference to a company or product name does not imply approval or recommendation of the product by the University of California or the U.S. Department of Energy to the exclusion of others that may be suitable.

TECHNICAL INFORMATION DEPARTMENT
LAWRENCE BERKELEY LABORATORY
UNIVERSITY OF CALIFORNIA
BERKELEY, CALIFORNIA 94720